TECHNISCHE MECHANIK, Band 23, Heft 1, (2003), 59-69
Manuskripteingang: 03. Februar 2003

Finite Element Simulation of Smart Lightweight Structures for Active Vibration and Interior Acoustic Control

J. Lefèvre, U. Gabbert

Dedicated to Dr.-Ing. Friedrich Wahl on the occasion of his 65th birthday.

The paper presents a numerical approach to active vibration and noise control of smart lightweight structures. The structure is provided with thin piezoelectric wafers as actuators and sensors to control vibrations of the structure. Fully coupled electromechanical field equations were taken into account where model based controllers are applied for design purposes. The objective of vibration control of elastic structures is to reduce interior noise levels. Hence, the mechanical field is also coupled with the acoustic field, and consequently a fully coupled electro-mechanical-acoustical problem needs to be solved. The numerical solution is based on the finite element method, introducing a velocity potential for the acoustic fluid to receive overall symmetric system matrices of the semi-discrete form of the equation of motion. It is shown that the vibro-acoustic coupling can be neglected for controller design purposes, and consequently the modal truncation technique considering only the uncoupled structural modes, can be adapted to vibro-acoustic systems. The behaviour of a smart plate structure coupled with an acoustic cavity is studied as a reference example.

1 Introduction

Over the past few years smart structural concepts have met with growing interest in many engineering branches and several new approaches and technologies have been developed (Tzou&Guran, 1998; Gabbert, 2002). Smart structures, or structronic systems, are characterized by a synergistic integration of active materials into a passive structure connected by a control system to facilitate automatic adjustment to changing environmental conditions. Piezoelectric materials are widely used as distributed sensors and actuators in smart structures. Commercially available piezoelectric wafers are commonly used as active materials for controlling structure vibrations. Such thin wafers may be glued on the surface of the base structure, or embedded in a composite material during the manufacturing process.

Intensified activities in developing and applying piezoelectric smart structures require effective and reliable design tools. The finite element method (FEM) is an excellent basis to develop powerful software tools. Being widely spread, it has become a theoretically and practically established method for solving coupled piezoelectric field problems. Based on the general purpose finite element software COSAR (COSAR, 1992), a tool has been designed and gradually implemented over the past few years (Berger et al., 2000; Gabbert et al., 2000). The software package contains an extended library of multi-field finite elements for 1D, 2D and 3D continua as well as for shell-type thin-walled structures (Seeger et al. 2002; Gabbert et al., 2002b). The COSAR FEM software is linked with controller design tools, such as MatLab/Simulink, through a general data interface, designing the controller on the basis of finite element models (Gabbert et al. 2001; Gabbert et al., 2002a).

Sound radiation is another major problem in designing engineering structures. Whenever an elastic structure gets into contact with a surrounding fluid, structural vibrations and the acoustic pressure field will influence each other. This vibro-acoustic coupling results in additional pressure loads on the structure-fluid interface caused by fluid pressure, as well as unwanted noise radiation caused by structural vibrations. Strong vibro-acoustic coupling effects occur in thin-walled lightweight structures of large surface. Active noise control by applying piezoelectric patch actuators to the structure is an alternative way to reduce noise radiation of elastic structures (see Balachandran et al., 1996; Ro&Baz, 1999; Kim et al., 1999; Gopinathan et al., 2000, and others).

Only recently, we extended our software tool COSAR by including new brick-type finite elements for discretizing acoustic volumes (Lefèvre, 2002). The velocity potential of the fluid was considered as an additional nodal degree of freedom in order to receive symmetric system matrices. Also, the vibro-acoustic coupling effect was taken into account. Now, it is possible to solve the fully coupled electro-mechanical-acoustic field problem on the basis of finite element discretization of the electromechanical structure and the fluid. Thermopiezoelectric effects as discussed by Görnandt et al., 2002, are neglected. Further below, the theoretical basis of this finite

element approach is presented, followed by a discussion of the controller design for vibro-acoustic problems. As large-scale finite element models cannot be used for controller design purposes, an appropriate model reduction is required to reduce the number of the degrees of freedom. Here, modal truncation seems to be the best suited method for establishing the controller design of structures based on the finite element discretization as flexible structures exhibit low-pass characteristics, which allow to neglect high-frequency dynamics (Straßberger, 1997). Based on selected eigenmodes the finite element model is reduced and transformed into the state space form. All required data of the modal state space model can be transferred to the controller design tool (MatLab/Simulink) via a general data exchange interface to design a suitable model-based controller. To study the controlled behaviour of the structure, the controller matrices can be retransferred to the original finite element model. As shown in the paper, adequate results can be received for controller design purposes by taking into account only the eigenmodes of the uncoupled structure. This procedure has been applied to interior acoustic problems with a strong fluid-structure interaction. The simulation of a smart rectangular elastic plate structure coupled with an acoustic cavity is investigated as a reference example.

2 Governing Equations and Finite Element Analysis

This section presents the theoretical background of our finite element software tool for simulating smart structures coupled with an acoustic fluid. First, the finite element analysis of coupled electromechanical structures and acoustic fluids are presented separately, followed by a demonstration how both approaches are coupled to receive an overall vibro-acoustic finite element model. The following equations are based on a Cartesian (x_1,x_2,x_3)-coordinate system.

2.1 Finite Element Model of Piezoelectric Smart Structures

The coupled electromechanical behaviour of a polarizable piezoelectric material in low voltage applications can be modelled with sufficient accuracy by means of linearized constitutive equations. Furthermore, small displacements are considered. The complete derivation of the finite element model is discussed in detail in Gabbert et al.(2000). Hence, only a brief summary of the equations is presented here.

In a three-dimensional continuum the finite element equations are based on the mechanical equilibrium

$$\mathbf{D}_u^T\boldsymbol{\sigma}+\bar{\mathbf{p}}=\rho\ddot{\mathbf{u}}\,, \tag{1}$$

the electric equilibrium (4th Maxwell equation)

$$\mathbf{D}_\varphi^T\mathbf{D}=0 \tag{2}$$

and the linear coupled electromechanical constitutive equations

$$\boldsymbol{\sigma}=\mathbf{C}\boldsymbol{\varepsilon}-\mathbf{e}\mathbf{E}\,, \tag{3}$$

$$\mathbf{D}=\mathbf{e}^T\boldsymbol{\varepsilon}+\boldsymbol{\kappa}\mathbf{E}\,, \tag{4}$$

with the stress vector $\boldsymbol{\sigma}^T=[\sigma_{11}\ \ \sigma_{22}\ \ \sigma_{33}\ \ \sigma_{12}\ \ \sigma_{23}\ \ \sigma_{31}]$, the body force vector $\bar{\mathbf{p}}^T=[\bar{p}_1\ \ \bar{p}_2\ \ \bar{p}_3]$, the displacement vector $\mathbf{u}^T=[u_1\ \ u_2\ \ u_3]$, the mass density ρ, the vector of electrical displacements $\mathbf{D}^T=[D_1\ \ D_2\ \ D_3]$ and the elasticity matrix $\mathbf{C}$[6×6], the piezoelectric matrix $\mathbf{e}$ [6×3], the dielectric matrix $\boldsymbol{\kappa}$ [3×3], the strain vector $\boldsymbol{\varepsilon}^T=[\varepsilon_{11}\ \ \varepsilon_{22}\ \ \varepsilon_{33}\ \ 2\varepsilon_{12}\ \ 2\varepsilon_{23}\ \ 2\varepsilon_{31}]$ and the electric field vector $\mathbf{E}^T=[E_1\ \ E_2\ \ E_3]$. $\mathbf{D}_u$ and $\mathbf{D}_\varphi$ describe the following differential matrix operators

$$\mathbf{D}_u^T=\begin{bmatrix}\frac{\partial}{\partial x_1} & 0 & 0 & \frac{\partial}{\partial x_2} & 0 & \frac{\partial}{\partial x_3}\\ 0 & \frac{\partial}{\partial x_2} & 0 & \frac{\partial}{\partial x_1} & \frac{\partial}{\partial x_3} & 0\\ 0 & 0 & \frac{\partial}{\partial x_3} & 0 & \frac{\partial}{\partial x_2} & \frac{\partial}{\partial x_1}\end{bmatrix} \tag{5}$$

and

$$\mathbf{D}_{\varphi}^{T}=\left[\frac{\partial}{\partial x_1}\quad\frac{\partial}{\partial x_2}\quad\frac{\partial}{\partial x_3}\right]. \tag{6}$$

Together with stress boundary conditions and the charge boundary conditions, the mechanical and the electric balance equations can be written in a weak form as

$$\chi=\int_V \delta\mathbf{u}^T\left(\mathbf{D}_u^T\boldsymbol{\sigma}+\overline{\mathbf{p}}-\rho\ddot{\mathbf{u}}\right)dV+\int_V \delta\varphi\left(\mathbf{D}_{\varphi}^T\mathbf{D}\right)dV+\int_{O_q}\delta\mathbf{u}^T\left(\overline{\mathbf{q}}-\mathbf{q}\right)dO+\int_{O_Q}\delta\varphi\left(\overline{Q}-Q\right)dO=0 \tag{7}$$

where $\delta\mathbf{u}$ is a virtual displacement, $\delta\varphi$ is a virtual electric potential, $\overline{\mathbf{q}}$ is a given traction vector on the surface O_q and $\overline{Q}$ is a given charge on the surface O_Q. In equation (7) the strain-displacement relation

$$\boldsymbol{\varepsilon}=\mathbf{D}_u\mathbf{u} \tag{8}$$

and the relation between the electric field and the electric potential

$$\mathbf{E}=-\mathbf{D}_{\varphi}\varphi, \tag{9}$$

are introduced. The displacements u_1, u_2, u_3 and the electric potential φ are approximated elementwise by shape functions, containing the element nodal parameters as unknown parameters. Including the shape functions of a finite element in the matrices $\mathbf{G}_u$ and $\mathbf{G}_{\varphi}$ and incorporating the unknown nodal parameters in the vectors $\mathbf{w}^{(e)}$ and $\boldsymbol{\varphi}^{(e)}$, the approximation of the displacement vector $\mathbf{u}$ and the electric potential φ can be written as

$$\mathbf{u}(x_1,x_2,x_3)=\mathbf{G}_u(x_1,x_2,x_3)\mathbf{w}^{(e)}, \tag{10}$$

$$\varphi(x_1,x_2,x_3)=\mathbf{G}_{\varphi}(x_1,x_2,x_3)\boldsymbol{\varphi}^{(e)}. \tag{11}$$

Following the standard finite element procedure, the semi-discrete form of the equations of motion of a general element (e) can be derived from equation (7) as follows

$$\begin{bmatrix}\mathbf{M}_{uu}^{(e)} & \mathbf{0}\\ \mathbf{0} & \mathbf{0}\end{bmatrix}\begin{bmatrix}\ddot{\mathbf{w}}^{(e)}\\ \ddot{\boldsymbol{\varphi}}^{(e)}\end{bmatrix}+\begin{bmatrix}\mathbf{K}_{uu}^{(e)} & \mathbf{K}_{u\varphi}^{(e)}\\ \mathbf{K}_{u\varphi}^{(e)T} & -\mathbf{K}_{\varphi\varphi}^{(e)}\end{bmatrix}\begin{bmatrix}\mathbf{w}^{(e)}\\ \boldsymbol{\varphi}^{(e)}\end{bmatrix}=\begin{bmatrix}\mathbf{f}_u^{(e)}\\ \mathbf{f}_{\varphi}^{(e)}\end{bmatrix}. \tag{12}$$

The vector $\mathbf{w}^{(e)}$ contains the nodal displacements and the vector $\boldsymbol{\varphi}^{(e)}$ contains the nodal electric potentials; $\mathbf{M}_{uu}^{(e)}$ is the element mass matrix, $\mathbf{K}_{uu}^{(e)}$ is the element stiffness matrix, $\mathbf{K}_{\varphi\varphi}^{(e)}$ is the element electric matrix, $\mathbf{K}_{u\varphi}^{(e)}$ is the piezoelectric coupling matrix, $\mathbf{f}_u^{(e)}$ is the load vector resulting from mechanical loads and $\mathbf{f}_{\varphi}^{(e)}$ is the load vector resulting from electric charges.

2.2 Finite Element Model of the Acoustic Fluid

Acoustic responses in a fluid are usually regarded as small perturbations related to an ambient reference state. Hence, the finite element model of the fluid is derived from the linear acoustic wave equation (Fahy, 1994)

$$\Delta p=\frac{1}{c^2}\ddot{p}, \tag{13}$$

considering the adiabatic wave propagation in a homogeneous, inviscid fluid. In equation (13) Δ is the Laplacian operator, p is the acoustic pressure and c is the sound speed. Although we are mainly interested in sound pressure distribution, the use of pressure p as a nodal variable is rather disadvantageous as in this case the finite element formulation of the coupled vibro-acoustic problem results in un-symmetric system matrices (Desmet&Vandepitte, 1999). Everstine (1997) recommended the introduction of the velocity potential Φ of the fluid as a new degree of freedom in order to obtain symmetric matrices. The velocity potential is a scalar field related to the velocity $\mathbf{v}$ of the fluid particles by

$$\mathbf{v} = -\mathbf{D}_a \Phi \tag{14}$$

and to the sound pressure by

$$p = \rho_0 \dot{\Phi}\,, \tag{15}$$

with the differential matrix operator $\mathbf{D}_a$, having the same form as the operator in equation (6), and the fluid density ρ_0 (Kollmann, 2000). Introducing equations (14) and (15) into equation (13) results in the new form of the acoustic wave equation

$$\Delta\Phi = \frac{1}{c^2}\ddot{\Phi}\,. \tag{16}$$

The next step considers an interior acoustic problem, i.e. the whole fluid volume is enclosed by boundaries in all directions with a finite distance from a common reference point. To obtain the weak form of the acoustic wave equation, equation (16) is multiplied by any test function τ and integrated over the fluid volume V_i. Using the Gaussian integral theorem the wave equation is derived in a weak form as

$$\int_{V_i} \tau\, \mathbf{D}_a^T \mathbf{D}_a \Phi \, dV + \int_{V_i} \frac{1}{c^2} \tau\, \ddot{\Phi}\, dV = \int_{O_i} \left(\tau\, \mathbf{D}_a^T \Phi\right) \mathbf{n}\, dO\,, \tag{17}$$

where $\mathbf{n}$ is the outward directed normal vector of the surface O_i of the volume V_i. The right hand side of equation (17) corresponds to the boundary conditions. O_i can be divided into the surfaces O_v with given normal velocity $\bar{v}_n$ and the surfaces O_z with an imposed impedance function $\bar{Z}_n$. The impedance function describes the relationship between the acoustic pressure and the normal component of the velocity

$$Z_n = \frac{p}{v_n}\,. \tag{18}$$

Following this procedure, it is possible to model boundary damping effects (Kim et al., 1999) and with the equations (14) and (15) equation (17) can be written as

$$\int_{V_i} \tau\, \mathbf{D}_a^T \mathbf{D}_a \Phi \, dV + \int_{V_i} \frac{1}{c^2} \tau\, \ddot{\Phi}\, dV = -\int_{O_v} \tau\, \bar{v}_n \, dO - \frac{\rho_0}{\bar{Z}_n} \int_{O_z} \tau\, \dot{\Phi}\, dO\,. \tag{19}$$

In a finite element the velocity potential Φ and the test function τ are approximated by using the vectors of the nodal degrees of freedom $\mathbf{\Phi}^{(e)}$, $\boldsymbol{\tau}^{(e)}$ and the matrix $\mathbf{G}_a$ containing the approximate functions as

$$\Phi\left(x_1, x_2, x_3\right) = \mathbf{G}_a\left(x_1, x_2, x_3\right)\mathbf{\Phi}^{(e)} \tag{20}$$

and

$$\tau\left(x_1, x_2, x_3\right) = \mathbf{G}_a\left(x_1, x_2, x_3\right)\boldsymbol{\tau}^{(e)}\,. \tag{21}$$

With the abbreviation

$$\mathbf{B}_a = \mathbf{D}_a \mathbf{G}_a\,, \tag{22}$$

and the equations (20) and (21) the equation (19) can be written as

$$\frac{1}{c^2} \int_{V_i^{(e)}} \boldsymbol{\tau}^{(e)T} \mathbf{G}_a{}^T \mathbf{G}_a \ddot{\mathbf{\Phi}}^{(e)} dV + \frac{\rho_0}{\bar{Z}_n} \int_{O_z^{(e)}} \boldsymbol{\tau}^{(e)T} \mathbf{G}_a^T \mathbf{G}_a \dot{\mathbf{\Phi}}^{(e)T} dO + \int_{V_i^{(e)}} \boldsymbol{\tau}^{(e)T} \mathbf{B}_a{}^T \mathbf{B}_a \mathbf{\Phi}^{(e)} dV = -\int_{O_v^{(e)}} \boldsymbol{\tau}^{(e)T} \mathbf{G}_a{}^T \bar{v}_n dO\,. \tag{23}$$

As this equation must to be fulfilled for any parameter $\boldsymbol{\tau}^{(e)}$ of the test function from equation (23) we receive

$$\mathbf{M}_a^{(e)} \ddot{\mathbf{\Phi}}^{(e)} + \mathbf{C}_a^{(e)} \dot{\mathbf{\Phi}}^{(e)} + \mathbf{K}_a^{(e)} \mathbf{\Phi}^{(e)} = \mathbf{f}_a^{(e)}, \tag{24}$$

with the acoustic element “mass” matrix

$$\mathbf{M}_a^{(e)} = \frac{1}{c^2} \int_{V_i^{(e)}} \mathbf{G}_a^T \mathbf{G}_a \, dV \,, \tag{25}$$

the acoustic element “damping” matrix

$$\mathbf{C}_a^{(e)} = \frac{\rho_0}{\bar{Z}_n} \int_{O_z^{(e)}} \mathbf{G}_a^T \mathbf{G}_a \, dO \,, \tag{26}$$

the acoustic element “stiffness” matrix

$$\mathbf{K}_a^{(e)} = \int_{V_i^{(e)}} \mathbf{B}_a^T \mathbf{B}_a \, dV \tag{27}$$

and the acoustic element “load” vector

$$\mathbf{f}_a^{(e)} = - \int_{O_v^{(e)}} \mathbf{G}_a^T \bar{v}_n \, dO \,. \tag{28}$$

2.3 Vibro-Acoustic Coupling

First, it is assumed that the acoustic pressure represents an additional load with respect to the structure. Developing our finite element model, we must also consider an additional load vector $\mathbf{f}_{uc}^{(e)}$ resulting from the acoustic pressure. Consequently, equation (12) can be augmented to

$$\begin{bmatrix} \mathbf{M}_{uu}^{(e)} & \mathbf{0} \\ \mathbf{0} & \mathbf{0} \end{bmatrix} \begin{bmatrix} \ddot{\mathbf{w}}^{(e)} \\ \ddot{\boldsymbol{\varphi}}^{(e)} \end{bmatrix} + \begin{bmatrix} \mathbf{K}_{uu}^{(e)} & \mathbf{K}_{u\varphi}^{(e)} \\ \mathbf{K}_{u\varphi}^{(e)T} & -\mathbf{K}_{\varphi\varphi}^{(e)} \end{bmatrix} \begin{bmatrix} \mathbf{w}^{(e)} \\ \boldsymbol{\varphi}^{(e)} \end{bmatrix} = \begin{bmatrix} \mathbf{f}_u^{(e)} + \mathbf{f}_{uc}^{(e)} \\ \mathbf{f}_{\varphi}^{(e)} \end{bmatrix}. \tag{29}$$

With equation (15) the vector $\mathbf{f}_{uc}^{(e)}$ can be calculated as

$$\mathbf{f}_{uc}^{(e)} = \int_{O_S^{(e)}} \mathbf{G}_u^T \mathbf{n} p \, dO = \rho_0 \int_{O_S^{(e)}} \mathbf{G}_u^T \mathbf{n} \mathbf{G}_a \, dO \, \dot{\boldsymbol{\Phi}}^{(e)} = \mathbf{C}_{uc}^{(e)} \dot{\boldsymbol{\Phi}}^{(e)}, \tag{30}$$

where O_s is the fluid structure interface and $\mathbf{C}_{uc}^{(e)}$ is the coupling matrix with regard to the acoustic pressure. Furthermore the velocity of the vibrating structure acts on O_s as a new acoustic load of the fluid

$$\mathbf{M}_a^{(e)} \ddot{\boldsymbol{\Phi}}^{(e)} + \mathbf{C}_a^{(e)} \dot{\boldsymbol{\Phi}}^{(e)} + \mathbf{K}_a^{(e)} \boldsymbol{\Phi}^{(e)} = \mathbf{f}_a^{(e)} + \mathbf{f}_{ac}^{(e)}. \tag{31}$$

Considering that the normal velocity of the structure can be expressed by

$$\dot{u}_n = \mathbf{n}^T \mathbf{G}_u \dot{\mathbf{w}}^{(e)}, \tag{32}$$

we receive an expression similar to equation (28)

$$\mathbf{f}_{ac}^{(e)} = - \int_{O_S^{(e)}} \mathbf{G}_a^T \mathbf{n}^T \mathbf{G}_u \, dO \, \dot{\mathbf{w}}^{(e)} = \mathbf{C}_{ac}^{(e)} \dot{\mathbf{w}}^{(e)}, \tag{33}$$

with $\mathbf{C}_{ac}^{(e)}$ as the coupling matrix regarding structural vibrations. Comparing equation (30) and equation (33), symmetric system matrices are received by multiplying all lines related to fluid degrees of freedom by ($-\rho_0$). Therefore and when the element matrices are included in a global matrix and the coupling matrices are inserted

in the left hand side, the semi-discrete system of equations of the electro-mechanical-acoustic field problem can be written as

$$\begin{bmatrix} \mathbf{M}_{uu} & \mathbf{0} & \mathbf{0} \\ \mathbf{0} & \mathbf{0} & \mathbf{0} \\ \mathbf{0} & \mathbf{0} & -\rho_0 \mathbf{M}_a \end{bmatrix} \begin{bmatrix} \ddot{\mathbf{w}} \\ \ddot{\boldsymbol{\varphi}} \\ \ddot{\boldsymbol{\Phi}} \end{bmatrix} + \begin{bmatrix} \mathbf{C}_{uu} & \mathbf{0} & -\mathbf{C}_{uc} \\ \mathbf{0} & \mathbf{0} & \mathbf{0} \\ -\mathbf{C}_{uc}^T & \mathbf{0} & -\rho_0 \mathbf{C}_a \end{bmatrix} \begin{bmatrix} \dot{\mathbf{w}} \\ \dot{\boldsymbol{\varphi}} \\ \dot{\boldsymbol{\Phi}} \end{bmatrix} + \begin{bmatrix} \mathbf{K}_{uu} & \mathbf{K}_{u\varphi} & \mathbf{0} \\ \mathbf{K}_{u\varphi}^T & -\mathbf{K}_{\varphi\varphi} & \mathbf{0} \\ \mathbf{0} & \mathbf{0} & -\rho_0 \mathbf{K}_a \end{bmatrix} \begin{bmatrix} \mathbf{w} \\ \boldsymbol{\varphi} \\ \boldsymbol{\Phi} \end{bmatrix} = \begin{bmatrix} \mathbf{f}_u \\ \mathbf{f}_\varphi \\ -\rho_0 \mathbf{f}_a \end{bmatrix}. \tag{34}$$

In equation (34) the Rayleigh damping has been introduced as the structural damping $\mathbf{C}_{uu}$. Mention should be made of the fact that the vector $\mathbf{w}$ also represents the nodal displacements of the passive part of the structure.

Based on equation (34) two acoustic brick-type elements with 8 and 20 nodes of the Serendipity element family have been developed and implemented in our COSAR software tool. The isoparametric element concept was used to properly approximate the element geometry. Furthermore, also the vibro-acoustic coupling procedures as presented in equations (29)-(30) were incorporated in the COSAR software tool. Together with initial conditions equation (34) can be integrated numerically, e.g. by using the Newmark formulas.

3 Control of Smart Structures

Numerical simulations of smart structures under the finite element concept require an overall finite element model comprising the passive structure, the active sensor and the actuator elements as well as a suitable model of the controller. Today, comprehensive design tools such as MatLab/Simulink are available to support the designing process. A general data exchange interface is required to exchange data and information between the finite element model and the controller design tool. Only recently, such data interface was developed to couple our finite element COSAR software with MatLab/Simulink (see Gabbert et al., 2001, 2002).

3.1 Controller Design

For controller design purposes the vibro-acoustic coupling effect is neglected in the active structure. Combining the displacement and the electric potential degrees of freedom in one vector

$$\overline{\mathbf{w}}^T = [\mathbf{w} \quad \boldsymbol{\varphi}], \tag{35}$$

equation (12) can be written as

$$\mathbf{M}\ddot{\overline{\mathbf{w}}} + \mathbf{C}\dot{\overline{\mathbf{w}}} + \mathbf{K}\overline{\mathbf{w}} = \overline{\mathbf{E}}\mathbf{f}(t) + \overline{\mathbf{B}}\mathbf{u}_r(t), \tag{36}$$

where $\mathbf{C}$ is an additional damping matrix and $\mathbf{u}_r$ (t) is the vector of the controller influence of the structure. The matrices $\overline{\mathbf{E}}$ and $\overline{\mathbf{B}}$ describe the positions of the external forces and the controller parameters in the finite element model, respectively. To use the modal truncation technique the linear eigenvalue problem

$$\left(\mathbf{K} - \omega_k^2 \mathbf{M}\right)\hat{\overline{\mathbf{w}}}_k = \mathbf{0}, \tag{37}$$

needs to be solved. The result is the modal matrix $\mathbf{Q} = \left[\hat{\overline{\mathbf{w}}}_1 \quad \hat{\overline{\mathbf{w}}}_2 \quad \ldots \quad \hat{\overline{\mathbf{w}}}_m\right]$, where m is the number of eigenmodes considered. Ortho-normalizing $\mathbf{Q}$ with $\mathbf{Q}^T\mathbf{M}\mathbf{Q} = \mathbf{I} = \mathrm{diag}(1)$ and $\mathbf{Q}^T\mathbf{K}\mathbf{Q} = \boldsymbol{\Omega} = \mathrm{diag}\left(\omega_k^2\right)$, we also obtain $\mathbf{Q}^T\mathbf{C}\mathbf{Q} = \boldsymbol{\Delta} = \mathrm{diag}\left(2\delta_k\omega_k\right)$, considering proportional damping. Introducing modal coordinates $\hat{\mathbf{q}}$ as

$$\overline{\mathbf{w}} = \mathbf{Q}\hat{\mathbf{q}} \tag{38}$$

into equation (36), we obtain the modal truncated system of (m×m) differential equations

$$\ddot{\hat{\mathbf{q}}} + \boldsymbol{\Delta}\dot{\hat{\mathbf{q}}} + \boldsymbol{\Omega}\hat{\mathbf{q}} = \mathbf{Q}^T\overline{\mathbf{E}}\mathbf{f}(t) + \mathbf{Q}^T\overline{\mathbf{B}}\mathbf{u}_r(t). \tag{39}$$

Equation (39) is transformed into the state space form, which is more convenient for the control theory. Introducing the state space vector

$$\mathbf{z} = \begin{bmatrix} \hat{\mathbf{q}} \\ \dot{\hat{\mathbf{q}}} \end{bmatrix} \tag{40}$$

in equation (39) results in

$$\dot{\mathbf{z}} = \begin{bmatrix} \mathbf{0} & \mathbf{I} \\ -\boldsymbol{\Omega} & -\boldsymbol{\Delta} \end{bmatrix} \mathbf{z} + \begin{bmatrix} \mathbf{0} \\ \mathbf{Q}^T \overline{\mathbf{B}} \end{bmatrix} \mathbf{u}_r(t) + \begin{bmatrix} \mathbf{0} \\ \mathbf{Q}^T \overline{\mathbf{E}} \end{bmatrix} \mathbf{f}(t) = \mathbf{A}_q \mathbf{z}(t) + \mathbf{B}_q \mathbf{u}_r(t) + \mathbf{E}_q \mathbf{f}(t) \ . \tag{41}$$

In smart structures a variety of signals can be measured, first of all electric potentials by using piezoelectric sensors; but also other signals, such as exiting forces or displacements, can be measured in order to characterize the state space of the structure. Hence, the measurement matrix is used in a general form as

$$\mathbf{y}(t) = \mathbf{C}_q \mathbf{z} + \mathbf{D}_q \mathbf{u}_r(t) + \mathbf{F}_q \mathbf{f}(t), \tag{42}$$

where $\mathbf{C}_q$, $\mathbf{D}_q$ and $\mathbf{F}_q$ are mapping matrices describing the relations between the measured quantities of the vectors $\mathbf{z}$, $\mathbf{u}_r$ and $\mathbf{f}$ with respect to the measuring vector $\mathbf{y}$. The matrices $\mathbf{A}_q$, $\mathbf{B}_q$, $\mathbf{E}_q$, $\mathbf{C}_q$, $\mathbf{D}_q$, $\mathbf{F}_q$ are transferred to MatLab/Simulink where the controller is designed. Designing a time independent LQ controller, the actuator signal is generated by the controller matrix $\mathbf{R}$ as

$$\mathbf{u}_r(t) = -\mathbf{R}\mathbf{z}(t). \tag{43}$$

3.2 Solution Concept

The semi-discrete form of the coupled vibro-acoustic equation of motion including control are as follows

$$\begin{bmatrix} \mathbf{M} & \mathbf{0} \\ \mathbf{0} & -\rho_0 \mathbf{M}_a \end{bmatrix} \begin{bmatrix} \ddot{\overline{\mathbf{w}}} \\ \ddot{\boldsymbol{\Phi}} \end{bmatrix} + \begin{bmatrix} \mathbf{C} & -\overline{\mathbf{C}}_{uc} \\ -\overline{\mathbf{C}}_{uc}^T & -\rho_0 \mathbf{C}_a \end{bmatrix} \begin{bmatrix} \dot{\overline{\mathbf{w}}} \\ \dot{\boldsymbol{\Phi}} \end{bmatrix} + \begin{bmatrix} \mathbf{K} & \mathbf{0} \\ \mathbf{0} & -\rho_0 \mathbf{K}_a \end{bmatrix} \begin{bmatrix} \overline{\mathbf{w}} \\ \boldsymbol{\Phi} \end{bmatrix} = \begin{bmatrix} \overline{\mathbf{E}}\mathbf{f}(t) + \overline{\mathbf{B}}\mathbf{u}_r(t) \\ -\rho_0 \mathbf{f}_a(t) \end{bmatrix}. \tag{44}$$

$\overline{\mathbf{C}}_{uc}$ is the coupling matrix with respect to the vector $\dot{\overline{\mathbf{w}}}$. To solve equation (44), the actuator signal (43) must be expressed in terms of $\overline{\mathbf{w}}$ and $\dot{\overline{\mathbf{w}}}$, respectively. If only a few selected eigenmodes are considered, $\mathbf{Q}$ is not a square matrix. To get the modal coordinates from equation (38), the pseudo-inverse matrix of $\mathbf{Q}$,

$$\mathbf{Q}^+ = \left(\mathbf{Q}^T \mathbf{Q}\right)^{-1} \mathbf{Q}^T \ , \tag{45}$$

is required. With equation (45) the state space vector has the following form

$$\mathbf{z} = \begin{bmatrix} \mathbf{Q}^+ \overline{\mathbf{w}} \\ \mathbf{Q}^+ \dot{\overline{\mathbf{w}}} \end{bmatrix}. \tag{46}$$

Mention should be made that the use of $\mathbf{Q}^+$ in equation (46) does not provide an exact solution with respect to the modal coordinates. However, if the motion of the structure is dominated by the selected eigenmodes, there is a very good agreement between the approach in equation (46) and the exact solution as we could establish. Following the integration procedure of the initial finite element model, the actuator signal $\mathbf{u}_r$ can be included as an additional force vector in the right hand side of equation (44).

4 Examples

This section contains a numerical demonstration of the fact that a controller designed with a modal reduced system as above can be applied with sufficient accuracy to a fully coupled vibro-acoustic system. The finite element

model of a clamped rectangular plate structure coupled with an acoustic cavity is used as a test example (Fig. 1). Four piezoelectric patches attached to the plate as two collocated actuator/sensor pairs (actuators on the top and sensors on the bottom of the plate) are employed. The structure is excited by a harmonic force at a given point. All dimensions and material properties of the plate, the acoustic cavity and the actuators/sensors are given in Tables 1 - 4. The plate is approximated by 96 passive hexahedron elements containing only mechanical degrees of freedom; the cavity is discretized with 384 acoustic hexahedron elements. Each actuator or sensor is approximated by a coupled piezoelectric hexahedron element containing mechanical as well as electrical degrees of freedom. In all these finite elements quadratic shape functions are used. The Newmark formulas are employed for numerical time integration of the equations of motion.

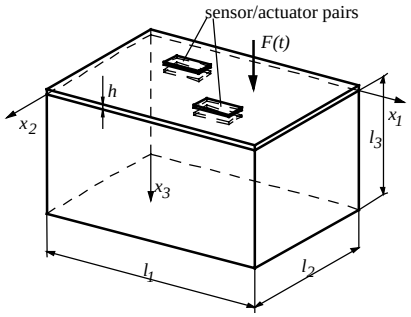

Figure 1. Smart Plate Structure Coupled with an Acoustic Cavity.

Plate/Cavity System		Actuators/Sensors	
l_1	600mm	Length in x_1-direction	100mm
l_2	400mm	Length in x_2-direction	50mm
l_3	400mm	Patch thickness	0.2mm
h (Plate thickness)	2mm		

Table 1. Geometry of the Vibro-acoustic System Including Actuators and Sensors.

Elastic Constants				Piezoelectric Constants		Dielectric Constants	
c_{11}	107600N/mm²	c_{33}	100400N/mm²	e_{15}	$1.20\cdot10^{-5}$N/(mV)mm	κ_{11}	$1.74\cdot10^{-14}$N/(mV)²
c_{12}	63120N/mm²	c_{44}	19620N/mm²	e_{31}	$-9.60\cdot10^{-6}$N/(mV)mm	κ_{33}	$1.87\cdot10^{-14}$N/(mV)²
c_{13}	63850N/mm²	c_{66}	22200N/mm²	e_{33}	$1.51\cdot10^{-5}$N/(mV)mm	Density ρ	$7.80\cdot10^{-9}$Ns²/mm^4

Table 2. Material Properties of the Piezoelectric Actuators and Sensors.

Young's modulus E	210000N/mm²
Poisson's ratio ν	0.3
Density ρ_P	$2.63\cdot10^{-9}$Ns²/mm^4

Table 3. Material Properties of the Elastic Plate.

Speed of sound c	340000mm/s
Fluid density ρ_0	$1.29\cdot10^{-12}$Ns²/mm^4

Table 4. Material Properties of the Acoustic Fluid.

Number	Frequency
1	47.3Hz
2	90.9Hz
3	143.6Hz
4	163.0Hz
5	193.4Hz

Table 5. Eigenfrequencies of the Uncoupled Elastic Plate.

In all simulations a force excitation with an amplitude of 1N and a frequency containing the first eigenfrequency (see Tab. 5) was applied, which is a very important excitation regarding the influence to the acoustic pressure in the enclosure. In the simulations the controller was switched on after a period of 1s. A LQ controller for the elastic plate was designed on the basis of a reduced model containing the first five structural modes (see Tab. 5). To verify the received controller matrix, the response of the plate was simulated without any vibro-acoustic coupling. Fig. 2 displays the resulting signal of the sensor.

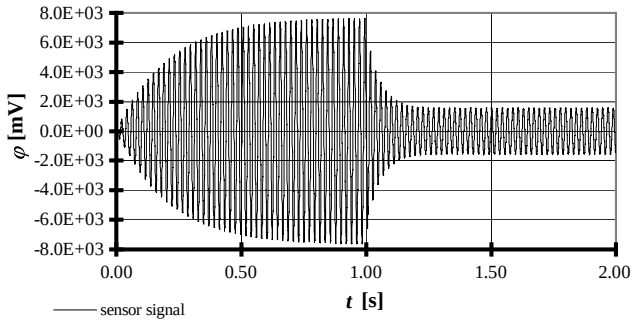

Figure 2. Sensor Signal of the Uncoupled Plate Resulting from Harmonic Excitation.

As can be seen in Fig. 2, the designed controller reduces structural vibrations to approximately a quarter of its maximum amplitude. The second simulation additionally considered the vibro-acoustic coupling. For this simulation the pressure release condition (p=0) was applied to all boundaries of the fluid in addition to coupling with an elastic plate, as included in the coupling equations (32) and (33). Fig. 3 displays the sensor signal.

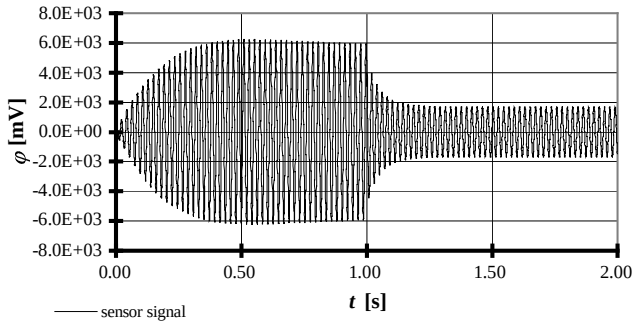

Figure 3. Resulting Sensor Signal with Respect to the Coupled Vibro-acoustic System under the Assumption of Boundary Pressure Release Conditions.

A comparison between Fig. 2 and Fig. 3 reveals that sound pressure does not exert a strong influence on the elastic plate when pressure release conditions are assumed at the boundaries. For the last simulation we assumed that the pressure release condition only acts on the boundary $x_3=l_3$. Apart from the plate all other four boundaries of the cavity were considered as acoustically hard surfaces (v_n=0). Fig. 4 displays the signal received by the sensors. Fig. 5 shows the corresponding sound pressure in the centre of the cavity. Fig. 4 and Fig. 5 display a strong coupling effect. The coupled fluid serves as an additional damping with respect to the vibrating plate. Furthermore, the motion of the plate is no longer only dominated by the first uncoupled eigenmode. The reason is the acoustic fluid altering the eigenfrequencies and eigenmodes of the whole system.

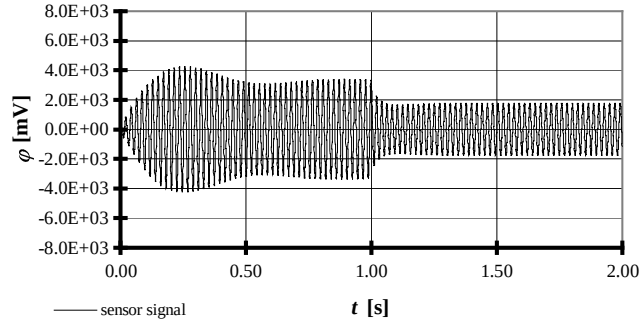

Figure 4. Resulting Sensor Signal of the Coupled Vibro-acoustic System Considering Acoustically Hard Boundaries.

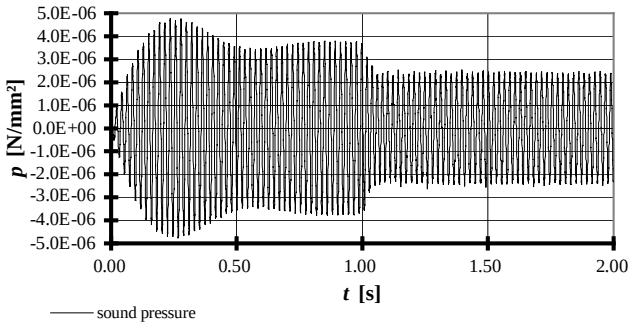

Figure 5. Resulting Sound Pressure in the Cavity Centre when Considering Acoustically Hard Boundaries.

As can be seen in all simulations, the controller reduces the sensor signals to almost the same level. In our opinion the fluid-structure interaction can be neglected for controller design purposes if there is no strong coupling between the structure and the fluid. However, we often encounter problems where a strong vibro-acoustic coupling occurs. Basically, the interaction of fluid and structure needs to be considered for controller design whenever a large surface area of a thin-walled lightweight structure is covered by a fluid. This is also of great importance when such models are used for calculating optimal actuator and sensor positions at the structure. In such cases the modal truncation should be based on the fully coupled electro-mechanical-acoustical eigenvalue problem.

5 Conclusions

The paper presents the theoretical background of a new finite element-based software tool for solving three-dimensional electro-mechanical-acoustical field problems, including control algorithms. This tool was incorporated in our finite element analysis software COSAR, facilitating simulations of the controlled behaviour of coupled vibro-acoustic systems with distributed piezoelectric actuators and sensors with regard to the interior acoustic radiation problem. A general data exchange interface is used to design controllers by MatLab/Simulink. Furthermore, numerical investigations were performed whether the modal truncation technique using the uncoupled structural modes for controller design can be adapted to vibro-acoustic systems. If there is no strong coupling between the fluid and the structure this method yields sufficient results. Otherwise, the eigenmodes of the completely coupled system need to be considered.

Acknowledgement

This work has been supported by the postgraduate program of the federal state of Sachsen-Anhalt. This support is gratefully acknowledged.

References

Balachandran, B., Samparth, A., Park, J.: Active control of interior noise in a three-dimensional enclosure, *J. of Smart Materials and Structures*, Vol. 5, (1996), pp. 89-97.

Berger, H., Gabbert, U., Köppe, H., Seeger, F.: Finite Element Analysis and Design of Piezoelectric Controlled Smart Structures, *J. of Theoretical and Applied Mechanics*, 3, 38, (2000), pp. 475-498.

COSAR – General Purpose Finite Element Package: *Manual*, FEMCOS mbH Magdeburg (see also http://www.femcos.de), (1992).

Desmet, W., Vandepitte, D.: Finite Element Method in Acoustics, *Proc. of the 10th International Seminar on Advanced Techniques in Applied and Numerical Acoustics*, Leuven, Belgium, (1999).

Everstine, G.C.: Finite Element Formulations of Structural Acoustic Problems, *J. Computers & Structures*, Vol. 65, No. 3, (1997), pp.307-321.

Fahy, F.: *Sound and Structural Vibration. Radiation, Transmission and Response*, Academic Press, London, (1994).

Gabbert, U., Berger, H., Köppe, H., Cao , X.: On Modelling and Analysis of Piezoelectric Smart Structures by the Finite Element Method, *J. of Applied Mechanics and Engineering*, Vol. 5, No. 1, (2000), pp. 127-142.

Gabbert, U., Köppe, H., Seeger, F.: Overall design of actively controlled smart structures by the finite element method, *SPIE Proceedings Series*, Vol. 4326, (2001), pp. 113-122.

Gabbert, U., Köppe, H., Nestorović Trajkov, T.: Entwurf intelligenter Strukturen unter Einbeziehung der Regelung. at – Automatisierungstechnik 50, 9, (2002a), pp. 432-438.

Gabbert, U., Köppe, H., Seeger, F., Berger, H.: Modeling of smart composite shell structures, *J. of Theoretical and Applied Mechanics*, 3, 40, (2002b), pp. 575-593.

Gabbert, U.: Research activities in smart materials and structures and expectations to future developments, *J. of Theoretical and Applied Mechanics*, 3, 40, (2002), pp. 549-574.

Görnandt, A., Gabbert, U. (2002): Finite Element Analysis of Thermopiezoelectric Smart Structures. *Acta Mechanica*, 154, (2002), pp. 129-140.

Gopinathan, S. V., Varadan, V. V., Varadan, V. K.: Finite Element/Boundary Element Simulation of Interior Noise Control Using Active-Passive Control Technique, *SPIE Proceedings Series*, Vol. 3984, (2000), pp. 22-32.

Kim, J., Ko, B., Lee, J.-K., Cheong, C.-C.: Finite element modeling of a piezoelectric smart structure for the cabin noise problem, *J. of Smart Materials and Structures*, Vol. 8, (1999), pp. 380-389.

Kim, J., Lee, J.-K., Im, B.-S., Chung, C.-C.: Modeling of Piezoelectric Smart Structures Including Absorbing Materials for Cabin Noise Problems, *SPIE Proceedings Series*, Vol. 3667, (1999), pp. 524-529.

Kollmann, F. G.: Maschinenakustik. Grundlagen, Meßtechnik, Berechnung, Beeinflussung, Springer-Verlag, Berlin-Heidelberg, (2000).

Lefèvre, J.: Modellierung und Simulation geregelter Leichtbaustrukturen zur aktiven Reduktion der Schallabstrahlung, Diplomarbeit, Otto-von-Guericke-Universität Magdeburg, Institut für Mechanik, (2002).

Ro, J., Baz, A.: Control of sound radiation from a plate into an acoustic cavity using active constrained layer damping, *J. of Smart Materials and Structures*, Vol. 8, (1999), pp. 292-300.

Seeger, F., Gabbert, U., Köppe, H., Fuchs, K.: Analysis and Design of Thin-Walled Smart Structures in Industrial Applications, *SPIE Proceedings Series*, Vol. 4698, (2002), pp. 342-350.

Straßberger, M.: Aktive Schallreduktion durch digitale Zustandsregelung der Strukturschwingungen mit Hilfe piezo-keramischer Aktoren, *Mitteilungen aus dem Institut für Mechanik*, Ruhr-Universität Bochum, (1997).

Tzou, H.-S., Guran, A. (Eds.): Structronic Systems: Smart Structures, Devices and Systems, Part 1: Materials and Structures, Part 2: Systems and Control, World Scientific, (1998).

Address: Dipl.-Ing. Jean Lefèvre, Prof. Dr.-Ing. habil. Dr. h. c. Ulrich Gabbert, Otto-von-Guericke-Universität Magdeburg, Universitätsplatz 2, D-39106 Magdeburg, e-mail: jean.lefevre@mb.uni-magdeburg.de, ulrich.gabbert@mb.uni-magdeburg.de